An Accurate Method for the PV Model Identification Based on a Genetic Algorithm and the Interior-Point Method

Dizqah, A. , Maheri, A. and Busawon, K.

Original citation:
Dizqah, AM, Maheri, A & Busawon, K, 2014, 'An accurate method for the PV model identification based on a genetic algorithm and the interior-point method', Renewable Energy, Vol. 72, pp 212–222
DOI: 10.1016/j.renene.2014.07.014

http://dx.doi.org/10.1016/j.renene.2014.07.014

Renewable Energy, 12/2014, vol.72, pp:212–222

An Accurate Method for the PV Model Identification Based on a Genetic Algorithm and the Interior-Point Method

Arash M. Dizqah[a,*], Alireza Maheri[a], Krishna Busawon[a]

[a]*Faculty of Engineering and Environment, University of Northumbria, NE1 8ST, Newcastle Upon Tyne, UK*

Abstract

Due to the PV module simulation requirements as well as recent applications of model-based controllers, the accurate photovoltaic (PV) model identification method is becoming essential to reduce the PV power losses effectively. The classical PV model identification methods use the manufacturers provided maximum power point (MPP) at the standard test condition (STC). However, the nominal operating cell temperature (NOCT) is the more practical condition and it is shown that the extracted model is not well suited to it. The proposed method in this paper estimates an accurate equivalent electrical circuit for the PV modules using both the STC and NOCT information provided by the manufacturers. A multi-objective global optimization problem is formulated using only the main equation of the PV module at these two conditions that restrains the errors due to employing the experimental temperature coefficients. A novel combination of a genetic algorithm (GA) and the interior-point method (IPM) allows the proposed method to be fast and accurate regardless the PV technology. It is shown that the overall error, which is defined by the sum of the MPP errors of both the STC and the NOCT conditions, is improved by a factor between 5.1% to 31% depending on the PV technology.

Keywords: Photovoltaic (PV), PV Model identification, Genetic algorithm (GA), Interior-point method (IPM), Maximum power point (MPP)

1. Introduction

Advances in PV technologies during the last decade have increased the share of the solar energy in the growing electricity market. The PV modules are nonlinear and complex still very popular components [1], [2] since they are easy to install and operate. However, it is essential to model the PV module accurately to be able to predict its behavior at different operating conditions. This PV behavioral prediction is necessary for the system design and the PV module simulation purposes (e.g. see [3]). Moreover, having an accurate model for the PV modules, it is also possible to develop the model-based MPPT algorithms (e.g. see [4]) besides the classic methods (e.g. see [5, 6, 7]).

A *PV cell* is a P-N junction that is typically modeled with an equivalent electrical circuit [8]. Although there are prior researches focused on non-electrical models based on either artificial neural network (ANN) [9] or adaptive neuro-fuzzy inference scheme (ANFIS) [10], the equivalent electrical circuit is the most popular PV model. The core advantage of the electrical models is that unlike the other models it does not necessarily require measured data samples to be trained. Moreover, it can easily be simulated with other components as an integrated electrical circuit. Fig. 1 illustrates a single-diode equivalent electrical circuit of the PV cell, which is also applicable to model a *PV module*. The PV module consists of several PV cells connected together in series. Although the double-diode circuit provides better modeling of the loss in the depletion region caused by the recombination of carriers [11]- [12], the single-diode model still offers

*Corresponding author
Email address: arash.moradinegade@northumbria.ac.uk (Arash M. Dizqah)

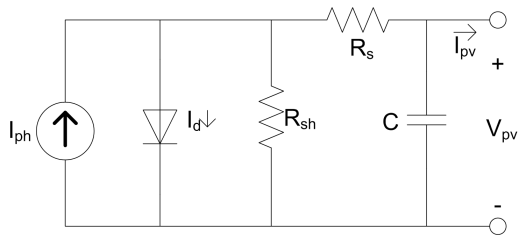

Figure 1: Single-diode equivalent electrical circuit of PV cell, module, and array.

a good compromise between accuracy and simplicity [13]. A *PV array,* which is a combination of several photovoltaic modules in series and parallel arrangement, can be modeled with the same circuit, too. There are six parameters in this model, namely, the stray capacitor C, the ideality factor of the diode n_d, the photocurrent I_{ph}, the reverse saturation current of the diode I_0, the series resistor R_s, and the shunt resistor R_{sh}. While the stray capacitor C is neglected [14], there are still five unknown parameters for each PV module, which require being determined with an identification method.

To the best of the authors knowledge, the prior researches on the PV electrical equivalent model identification methods can be categorized into three groups. Each of these methods can also be applied to either a simplified model taken the shunt resistor as infinite [15], [16] or the normal circuit leading to a four- or five-parameter estimation problem, respectively.

In the first group, the authors in [17, 18, 19, 20, 21] presented analytical methods to calculate the parameters. The identification method proposed in [17] attempts to approximate and solve analytically the equation of the PV as a polynomial of the first order. Even though a simple parameter estimation method is demonstrated, the method does not provide enough accuracy. The works of [18, 19, 20, 21], however, introduced a system of five equations to resolve the five model parameters. Three of these equations are extracted from three remarkable points [13], i.e., the short- and the open-circuit points coupled with the MPP. While the forth equation is constructed based on the fact that the derivative of the power at the MPP is zero, the fifth equation is more challenging. The authors in [18] employed an approximation for the temperature coefficient as the fifth equation, however, the others adopt the equation introduced in [19] as a simplified approximation of the shunt resistor. Although these analytical methods are straightforward and only need the nominal values from datasheets, they still need sophisticated numerical or even optimization methods to solve the resulting nonlinear and transcendental system of equations. Moreover, the accuracy is deteriorated as a result of using simplified approximation of either the temperature coefficient or the shunt resistor.

Alternatively, there are prior researches focused on identifying a PV current-voltage ($I-V$) curve (Fig. 2) being the best fit to the empirical data [22, 23, 24, 25]. The authors in [22] and [23] proposed a genetic algorithm as the curve fitting procedure to identify the circuit in Fig. 1. The main issue of this approach is that it relies on measured data rather than information available in datasheets. Moreover, it requires measuring the cell temperature of the PV module, which is not an easy task. With the aim of avoiding the need to measure points on the different $I-V$ curves, the authors in [24] introduced a set of equations to calculate the remarkable as well as two intermediate points at different values of the insolation and the cell temperature. This method is adopted by Sandia national laboratories (SNL), USA [26] as the reference method in PV model identification. The equations rely on several empirical parameters, which need to be extracted for each type of the PV module. The national institute of standards and technology (NIST), USA [27] provides these empirical parameters for different PV module technologies [18]. The procedure needs to be repeated for any new PV module type.

Finally, in order to avoid issues of these approaches, i.e., the needs for measuring points on the $I-V$ curves and degrading the accuracy caused by the simplifications, the authors in [13], and [28] proposed methods based on optimization techniques. The identification method proposed in [13] employed an exhaustive search algorithm to explore all values of the ideality factor and the series resistor. It calculates the value of the shunt resistor iteratively. Although it is an effective algorithm, it requires checking all possible values of the

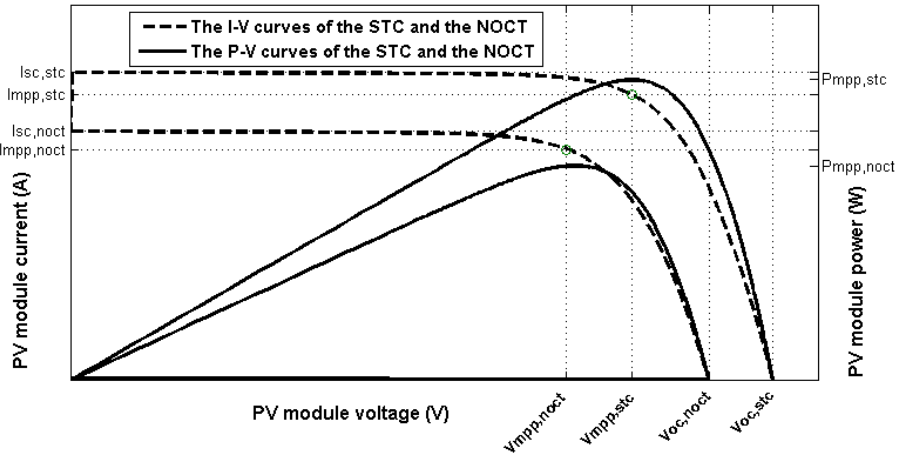

Figure 2: The $I-V$ and $P-V$ curves of the PV module for the STC and the NOCT conditions.

ideality factor and the series resistor before determining the optimal ones as well as calculating a complete $I-V$ curve at each iteration. These two issues make the procedure quite slow. Furthermore, the speed of the procedure is sensitive to the resolution of the parameters with the order of $O\left(\left(\frac{resolution_{new}}{resolution_{old}}\right)^2\right)$. The authors in [28] reformulated the problem as an unconstrained optimization problem. Then they employed the particle swarm optimization (PSO) technique to solve it at different values of the cell temperature. Although the formulation and the employed algorithm increase the speed of the procedure, it still requires solving the $I-V$ as well as two other transcendental equations at each iteration, which degrade the speed.

The main limitations of these methods are that they either require experimental measurements or use only the STC information available in datasheets. In order to fit the experimental points to a mathematical presentation of an $I-V$ curve, it requires measuring the cells temperature, i.e. the P-N junction temperature of packed PV cells, and keeping them constant during the test which both are not easy to handle. Meanwhile, the STC information estimates parameters with good accuracy for the MPP at the STC; however, as shown in subsection 3.3, it introduces a considerable error for the MPP at the NOCT. Furthermore, the methods based on the optimization techniques solve repeatedly the nonlinear transcendental $I-V$ curve for the whole range of the PV voltage and it causes them to be slow. To overcome these limitations, this paper proposes a novel PV model identification method to estimate the electrical parameters with minimum *overall error*, namely, the *overall optimum solution*. The overall error is defined by the sum of the STC and NOCT errors, which are the MPP estimation errors for the STC and NOCT curves, respectively. In this paper, the proposed method is applied for extracting the electrical parameters of the equivalent single-diode circuit; however, with some modifications it is also applicable to the double-diode model of a PV module. The proposed method relies on a multi-objective optimization problem (MOOP) using either any empirical inaccurate equations or any assumptions on the parameters. A novel combination of a Genetic algorithm (GA) and the interior-point method (IPM) is introduced to solve the resulting MOOP in considerably short time. It is shown that the overall error is improved for three PV technologies, i.e. thin film, polycrystalline, or monocrystalline technologies. The results are also compared with the results of two prior researches [13, 28] that shows improvement in terms of overall and STC errors. Moreover, by employing IPM, the proposed method is faster than the method introduced in [13].

This paper is organized as follows: the next section provides a summary of the PV mathematical model. Section III presents a formulation of the MPP estimation and parameter identification problems as well as the proposed procedure. The identified electrical parameters for three different PV technologies coupled with their validation are given in Section IV. Finally, Section V presents a conclusion of the study. Fig. 3 provides a summary of the manuscript indicating different stages of the proposed PV model identification and validations procedure. As it is depicted, the available STC and NOCT information provided by man-

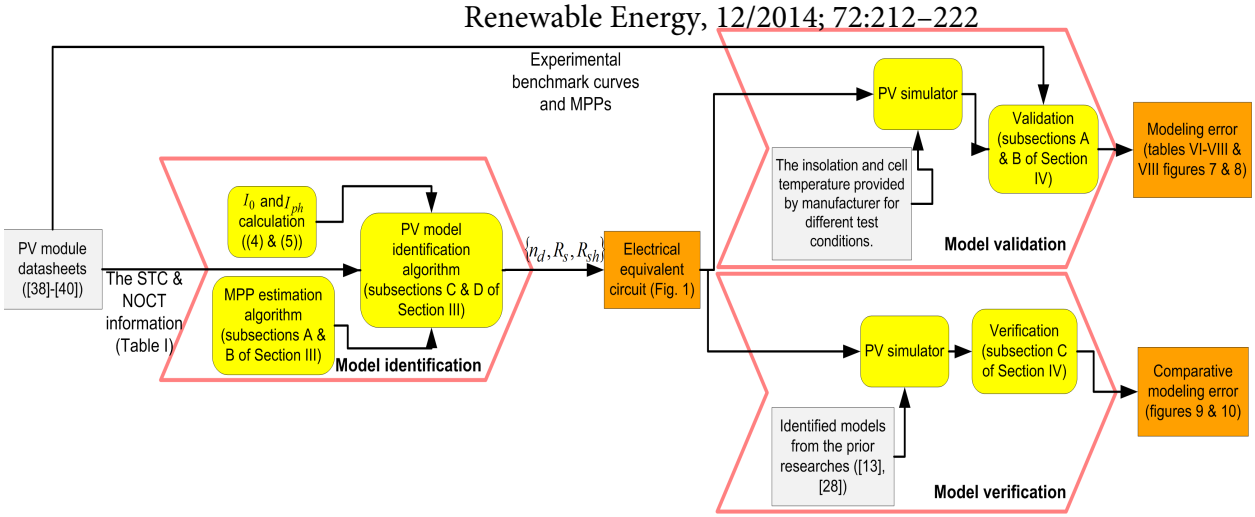

Figure 3: An outline of the manuscript indicating different stages of the proposed procedure.

ufacturers are used by the proposed algorithm to identify the $\{n_d, R_s, R_{sh}\}$ parameters of the PV module equivalent electrical circuit. The identified electrical model is then validated against available $I-V$ curves and MPPs information provided by manufacturer. The differences between the simulated PV curves and MPPs and those from datasheets, i.e. modeling errors, are also compared with the similar results reported by prior researches.

2. PV module mathematical modeling

Fig. 1 illustrates a single-diode equivalent electrical circuit of a PV module. Among the electrical parameters, the series resistor R_s is the sum of structural resistances [13] and the shunt resistor R_{sh} representing the leakage current [13]. Applying the Kirchhoff current law (KCL) to the junction point of these two resistors gives the characteristic equation of the PV module, which is a nonlinear transcendental equation, as follows:

$$I_{pv} = I_{ph} - I_0 \left\{ \exp\left(\frac{V_{pv} + R_s I_{pv}}{n_d N_s} \frac{q}{K T_c}\right) - 1 \right\} - \frac{V_{pv} + R_s I_{pv}}{R_{sh}}. \tag{1}$$

where V_{pv} and I_{pv} are, respectively, the output voltage and current of the PV module and all other symbols are defined as follows:

- q The electron charge (1.60218×10^{-19})
- K The Boltzman constant (1.38066×10^{-23})
- N_s The number of the PV cells in series constructing the PV module (-)
- T_c The current amount of the PV cell temperature (K)

The photocurrent I_{ph} and the reverse saturation current of the diode I_0 for the STC and the NOCT conditions are calculated using available parameters in the datasheets [13], [29]:

$$I_{ph} = \left(\frac{R_s + R_{sh}}{R_{sh}} I_{sc,X} + k_I \left(T_c - T_{c,X}\right) \right) \frac{S}{S_X}. \tag{2}$$

$$I_0 = \frac{I_{sc,X} + k_I \left(T_c - T_{c,X}\right)}{\exp\left(\frac{V_{oc,X} + k_V \left(T_c - T_{c,X}\right)}{n_d N_s} \frac{q}{K T_c}\right) - 1}. \tag{3}$$

$I_{sc,X}$ The short-circuit current of the PV module at condition X (A)
k_I The temperature coefficient of the short-circuit current ($A/^\circ C$)
k_V The temperature coefficient of the open-circuit voltage ($V/^\circ C$)
S The current amount of the solar irradiance (W/m^2)
S_X The standard amount of the solar irradiance at condition X (W/m^2)
$T_{c,X}$ The standard amount of the cell temperature at condition X (K)
$V_{oc,X}$ The open-circuit voltage of the PV module at condition X (V)
X The operating condition that is either the STC or the NOCT (-)

where the parameters are defined as follows:

Manufacturers provide all the above parameters, i.e., the empirical values of the remarkable points for each operation conditions as well as the cell temperature at the NOCT. Table 1 illustrates these information for the PV modules studied in this paper.

Under the STC and the NOCT conditions, Eqs. (2) and (3) can be rewritten as follows:

$$I_{ph} = \begin{cases} \dfrac{R_s + R_{sh}}{R_{sh}} I_{sc,stc} & \text{For the STC-curve,} \\ \dfrac{R_s + R_{sh}}{R_{sh}} I_{sc,noct} & \text{For the NOCT-curve.} \end{cases} \tag{4}$$

$$I_0 = \begin{cases} \dfrac{I_{sc,stc}}{\exp\left(\dfrac{V_{oc,stc}}{n_d N_s} \dfrac{q}{K T_{c,stc}}\right) - 1} & \text{For the STC-curve,} \\ \dfrac{I_{sc,noct}}{\exp\left(\dfrac{V_{oc,noct}}{n_d N_s} \dfrac{q}{K T_{c,noct}}\right) - 1} & \text{For the NOCT-curve.} \end{cases} \tag{5}$$

By substituting Eqs. (4) and (5) into Eq.(1), one obtains the equations of the two $I - V$ curves in Fig. 2, which their stationary points are the MPPs.

There are other equations to model the deviation of the photocurrent, the short-circuit current, and the open-circuit voltage due to a variation in the cell temperature [18], [28]. None of these equations are used in the proposed method and it only uses Eq. (1) under the STC and the NOCT conditions to increases the accuracy of the method.

Table 1: PV modules studied in this paper and their datasheet information.

	Polycrystalline	**Thin film**	**Monocrystalline**
Parameters	**KC200GT (Kyocera)**	**ST40 (SHELL)**	**E20/333 (Sunpower)**
$I_{mpp,stc}$	$7.61(A)$	$2.41(A)$	$6.09(A)$
$V_{mpp,stc}$	$26.3(V)$	$16.6(V)$	$54.7(V)$
$P_{mpp,stc}$	$200.143(W)$	$40.00(W)$	$333.123(W)$
$I_{sc,stc}$	$8.21(A)$	$2.68(A)$	$6.46(A)$
$V_{oc,stc}$	$32.9(V)$	$23.3(V)$	$65.3(V)$
$I_{mpp,noct}$	$6.13(A)$	$1.88(A)$	$4.91(A)$
$V_{mpp,noct}$	$23.2(V)$	$14.7(V)$	$50.4(V)$
$P_{mpp,noct}$	$142.216(W)$	$27.7(W)$	$247.64(W)$
$I_{sc,noct}$	$6.62(A)$	$2.2(A)$	$5.22(A)$
$V_{oc,noct}$	$29.9(V)$	$20.7(V)$	$61.2(V)$
k_I	$3.18 \times 10^{-3}(A/^\circ C)$	$0.35 \times 10^{-3}(A/^\circ C)$	$3.5 \times 10^{-3}(A/^\circ C)$
k_V	$-1.23 \times 10^{-1}(V/^\circ C)$	$-100 \times 10^{-3}(V/^\circ C)$	$-176.6 \times 10^{-3}(V/^\circ C)$
N_s	54	36	96
$T_{c,noct}$	$47^\circ C$	$47^\circ C$	$45^\circ C$
$T_{c,stc}$	$25^\circ C$	$25^\circ C$	$25^\circ C$

3. Problem formulation

PV model identification is an optimization problem to find the optimum parameters for the equivalen electrical model of a PV module in terms of minimizing some identification errors. However, there are two main challenges. First, this section shows that PV model identification is an optimization problem with multiple local optima points that must be solved to find its global optimum point. Moreover, it is shown that estimating the electrical parameters, in the way that the MPPs of both STC and NOCT curves are matched with manufacturers data, are conflicting objectives. Therefore, the PV model identification is formulated as a global MOOP with two constraints on the MPPs of the STC and the NOCT curves. A specific GA is proposed to solve this global MOOP. It relies on a fast MPP estimation algorithm, explained below, that employs the IPM.

3.1. Formulating the MPP estimation problem

The MPP is the point (V_{mpp}, I_{mpp}) on the $I-V$ curve that maximizes the produced power of the PV module. As a result, the problem of estimating the MPP for either the STC- or the NOCT-curve can be formulated as follows:

$$[V_{mpp}, I_{mpp}] = \arg \underset{\mathrm{v_{pv}}, \mathrm{i_{pv}} \in \Re}{\text{minimize}} \left\{ \frac{1}{v_{pv} i_{pv}} \right\} \tag{6a}$$

subject to:

$$i_{pv} = i_{ph} - i_0 \left\{ \exp(\frac{v_{pv} + R_s i_{pv}}{n_d N_s} \frac{q}{K T_c}) - 1 \right\} - \frac{v_{pv} + R_s i_{pv}}{R_{sh}} \tag{6b}$$

$$i_{ph} = \frac{R_s + R_{sh}}{R_{sh}} I_{sc} \tag{6c}$$

$$i_0 = \frac{I_{sc}}{\exp(\frac{V_{oc}}{n_d N_s} \frac{q}{K T_c}) - 1} \tag{6d}$$

$$0 \leq [v_{pv}, i_{pv}]^T \leq [V_{oc}, I_{sc}]^T. \tag{6e}$$

Given the PV module information for the test conditions of the Table 1 and the electrical parameters of the Fig. 1, the MPP can be estimated for either of the test conditions. The objective function, which needs to be minimized, is the reverse of the generated power. There is a nonlinear constraint (6b) that is the $I-V$ curve of the PV module. Except the box constraints (6e) the others provide the equations to calculate the photocurrent and the diode reverse saturation current.

3.2. The proposed MPP estimation algorithm

The optimization problem (6) can be solved employing either the curve-inspecting technique, the local optimization methods, or even the heuristic algorithms such as a GA. The authors in [12], [13], and [28] employed the curve-inspecting method, which is an exhaustive search method, to find the MPP of the $I-V$ curve. This algorithm solves the transcendental Eq. (6b) for I_{pv} with respect to all possible values of V_{pv} with a Newton-Raphson based method. Then, it finds the MPP as the couple (V_{mpp}, I_{mpp}) generating the maximum power. The procedure needs to calculate a complete $I-V$ curve to be able to extract the MPP and its speed depends significantly on the step-size of the V_{pv} variation.

From Fig. 2, it can be seen that the generated power by the PV module is a concave function with respect to the PV voltage ($P-V$ curve). Consequently, the objective function of the problem (6) is convex over the feasible values of V_{pv} and I_{pv} and it can be solved employing well-known nonlinear convex optimization techniques. In this study, the IPM, which is also known as the barrier method, has been selected chiefly because it solves the problem faster comparing with the curve-inspecting method. Furthermore, there exists a powerful still freely accessible implementation of the IPM, i.e., the interior point optimizer (IPOPT) [30].

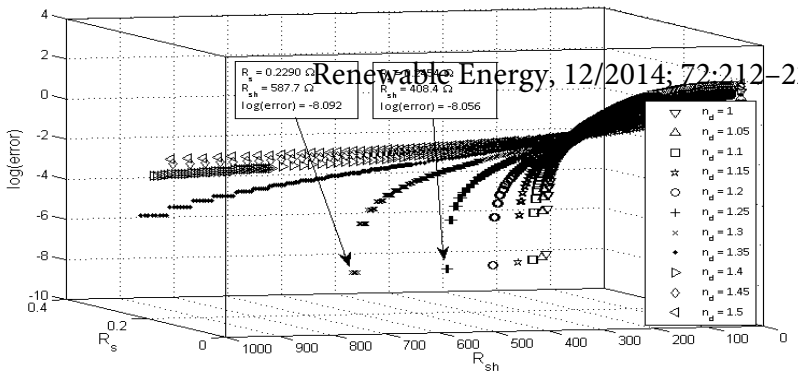

Figure 4: The existance of local optima for different values of the ideality factor.

In contrast to many other optimization techniques, IPM traverses the interior points inside the boundaries to find the optimal solution.

The fundamental idea of the IPM is to transform the nonlinear optimization problem with inequality constraints to a problem with only equality constraints. Then the optimum value is estimated through satisfying the necessary conditions proposed by the Karush-Kuhn-Tucker (KKT) theorem. A summary of the IPM is provided in the Appendix I and for further details, the reader is referred to [31] and [32].

Table 2 summarizes the execution time of the curve-inspecting and the proposed methods to solve the problem (6). It illustrates that the curve-inspecting technique is computationally quite expensive. While the implementation of the proposed MPP estimation algorithm in MATLAB is more than 10 times faster, employing the IPOPT makes it even much faster. The MPP estimation is a critical task of the PV module identification because it is executed several times depending on the identification algorithm and its parameters, e.g., the population size and the maximum number of generations in a GA. A fast MPP estimation algorithm, in particular, speeds up the identification algorithm, explained below, substantially.

3.3. Formulating the PV model identification problem

PV module manufacturers report the maximum power points at two different conditions, namely, STC and NOCT conditions, in their datasheets. In this paper, the PV model identification problem has been extended as the procedure of identifying the best values for n_d, R_s, and R_{sh} parameters (Fig. 1) such that not only the $I-V$ curve (Eq. (1)) at the STC condition but also the appropriate $I-V$ curve at the NOCT condition have the maximum output power as much similar as possible to the $(V_{mpp}$,$I_{mpp})$ points reported by the manufacturers (Table 1). Identifying these parameters, Eqs. (2), and (3) can be employed to calculate the remaining I_{ph}, and I_0 parameters.

Fig. 4 illustrates the *identification errors* for different values of the ideality factor. They have been depicted just up to the optimum points for simplicity's sake. This identification error is the absolute difference between the estimated MPP and the MPP provided by the manufacturer and is defined by a normalized Euclidean distance. In Fig. 4, it can be seen that for each individual value of the ideality factor there is a local optimum with respect to other model parameters R_s and R_{sh} and this fact introduces multiple local optima to the problem. For instance, when n_d equals to 1.25, which is illustrated by "+" comparing for example to the case of $n_d = 1.5$ illustrated by "$\lhd$", the local optima locates at $(R_s, R_{sh}) = (0.2454\Omega, 408.4\Omega)$ and the relevant error is -8.056.

Table 2: The execution time of different methods to estimate the MPP.

Methods	**The execution time**
The curve-inspecting method with MATLAB	3000($msec$)
The proposed algorithm with MATLAB	300($msec$)
The proposed algorithm with IPOPT	90($msec$)

Table 3: Conflicts between the STC- and the NOCT-based objectives.

PV modules $\longrightarrow$	**KC200GT**		**ST40**	
Error Type $\downarrow$	**Parameters of [13]**	**Using NOCT-based objective**	**Parameters of [28]**	**Using NOCT-based objective**
STC-identification error	0.00262	0.03192	0.00499	0.03214
NOCT-identification error	0.02401	0.00003	0.05166	0.00002

Based on available STC and NOCT MPPs provided by manufacturers , two varieties of the identification errors are defined. These *STC-identification* and *NOCT-identification* errors measure the difference between the calculated MPPs by an identified model and MPPs reported in datasheets for the STC and NOCT conditions. Although the prior researches (e.g. [13] and [28]) used the STC information available in datasheets, the NOCT data can also be employed for PV model identification purpose. Table 3 compares these two approaches in terms of STC- and NOCT-identification errors. From Table 3, it can be seen that minimizing either of these errors does not minimize the other one. For instance, the identified PV model based on available NOCT information in KC200GT PV module datasheet, instead of the STC information, decreases the NOCT-identification error but increases the STC-identification error. In other words, the identified model that proposes an optimum point for the STC-identification error does not provide an optimum point for the NOCT-identification error and vice versa. Therefore, considering both the STC and the NOCT conditions introduce a MOOP [33] with the following conflicting objectives:

$$J_1(v_{pv}, i_{pv}) = \|[\frac{v_{pv} - V_{mpp,stc}}{V_{mpp,stc}}, \frac{i_{pv} - I_{mpp,stc}}{I_{mpp,stc}}, \frac{v_{pv}i_{pv} - P_{mpp,stc}}{P_{mpp,stc}}]\|_2. \tag{7}$$

$$J_2(v_{pv}, i_{pv}) = \|[\frac{v_{pv} - V_{mpp,noct}}{V_{mpp,noct}}, \frac{i_{pv} - I_{mpp,noct}}{I_{mpp,noct}}, \frac{v_{pv}i_{pv} - P_{mpp,noct}}{P_{mpp,noct}}]\|_2. \tag{8}$$

$$J(v_{pv}, i_{pv}) = \{w_1\theta_1 J_1(v_{pv}, i_{pv}) + w_2\theta_2 J_2(v_{pv}, i_{pv})\}. \tag{9}$$

Due to the fact that the power is the multiplication of the voltage and the current, considering only the generated power in the objective functions and discarding these two factors introduces an algorithmic error. Moreover, Eq. (10) indicates that even small amount of round-off error in the estimated V_{mpp} and I_{mpp}, namely, ε_v and ε_i are magnified by the values of the voltage and current before taking into account as the estimated P_{mpp} error, ε_p. In order to eliminate these issues, the difference between all these three factors and the nominal values available in datasheets have been considered.

$$\varepsilon_p = V_{mpp}\varepsilon_i + I_{mpp}\varepsilon_v. \tag{10}$$

Although the open- and short-circuit points can also be added as parts of the objective functions, it is unnecessary because they are considered in Eqs. (4) and (5). Fig. 6 of next section shows that the$I - V$ curve of the estimated parameters for the STC condition passes through all remarkable points accurately.

There are two approaches to solve the multi-objective optimization problems: converting to a single-objective problem, and determining the entire Pareto solution [34]. While the former approach returns a single solution, the latter provide a Pareto optimal set as a set of solutions that are not dominated with each other. The decision-maker selects among the Pareto optimal set according to trade-offs. The proposed algorithm in this paper without loss of generality employs the first approach for two reasons. While it is easier to implement, the proposed algorithm also aims at estimating the best set of values for the parameters rather than a set of optimal solutions.

The individual objectives (7) and (8) are converted to a single objective (9) employing a weighted affine combination of the normalized objective functions $\hat{J} = \left[\hat{J}_1, ..., \hat{J}_k\right]$ with weights $w = [w_1, ..., w_k]^T$ [34]. The

Table 4: The box constraints of the electrical parameters.

Parameters	**KC200GT**	**ST40**	**E20/333**
$n_{d,\min}(-)$	1.0	1.0	1.0
$n_{d,\max}(-)$	2.0	2.0	2.0
$R_{s,\min}(\Omega)$	0.001	0.001	0.001
$R_{s,\max}(\Omega)$	1.0	1.0	2.0
$R_{sh,\min}(\Omega)$	50	50	50
$R_{sh,\max}(\Omega)$	1100	550	1500

affine combination means that $\sum_{i=1}^{k} w_i = 1$ and the normalized objective function is defined as follows:

$$\hat{J} = [\theta_1, ...\theta_k]^T [J_1, ..., J_k] \tag{11a}$$

$$\theta_i = \frac{1}{f_i(x^{[i]})} \tag{11b}$$

$$x^{[i]} = \arg \underset{\mathrm{x}\in\chi}{\text{maximize}} \quad \{f_i(x)\}\,. \tag{11c}$$

where k is the number of individual objective functions. In order to keep the values of all objective functions in the range of $[0, 1]$, the normalization factors $\{\theta_i\}$ are selected as the reverse of the maximum value of each objective function (11b). The resulting single-objective PV model identification problem is proposed as follows:

$$[R_{s,opt}, R_{sh,opt}, n_{d,opt}] = \arg \underset{\mathrm{R_s},\mathrm{R_{sh}},\mathrm{n_d}\in\Re}{\text{minimize}}$$

$$\{w_1\theta_1 J_1(v_{mpp,stc}, i_{mpp,stc}) + w_2\theta_2 J_2(v_{mpp,noct}, i_{mpp,noct})\} \tag{12a}$$

subject to:

$$[v_{mpp,stc}, i_{mpp,stc}] = \text{The solution of (6) for the STC} \tag{12b}$$

$$[v_{mpp,noct}, i_{mpp,noct}] = \text{The solution of (6) for the NOCT} \tag{12c}$$

$$[R_{s,min}, R_{sh,min}, n_{d,min}]^T \leq [R_s, R_{sh}, n_d]^T \leq [R_{s,max}, R_{sh,max}, n_{d,max}]^T. \tag{12d}$$

Through this study, the normalization factors are calculated dynamically and the weights are assumed to be equal (i.e. $[0.5, 0.5]$). The proposed method for this case can be named as the *full method*. The equal weights imply that there is no preferences between either of the STC or the NOCT conditions, however, if there is such a preference the affine weights can be unbalanced. Particularly, applying either of the values of $[1, 0]$ or $[0, 1]$ convert Eq. (12) to a single (only Eq. (7) or Eq. (8)) objective problem and the proposed method can be called the *STC- or NOCT-based method*. The two constraints (12b) and (12c) present the MPPs of the STC and NOCT curves according to Eq. (6). Table 4 summarizes the box constraints of the electrical parameters for the different PV modules studied in this paper.

3.4. The proposed PV model identification algorithm

The well-known nonlinear programming (NLP) algorithms such as IPM cannot solve the PV model identification problem (12) since it is a global optimization problem with multiple local optima. To address this problem, a GA is proposed in this paper.

Generally speaking, a GA is a search technique based on the natural genetic mechanisms. It is a class of stochastic search methods combining elements of two strategies, namely, exploring the search space and exploiting the best solution [35]. The GAs start with an initial fixed-size population, which is a set of random individual chromosomes, representing a string of the values of design variables. New offsprings are generated by either a crossover or a mutation operation. The chromosomes evolve through the generations according to a selection rule states that the fitter chromosomes have higher probabilities of being selected [35].

Table 5: The pseudocode of the proposed PV model identification method.

Step1: Initialization

Load the optimization parameters: popSize, genNo_max, mutRate_init, crossoverRate;
Load the PV parameters from datasheets;
$genIndx = 0$; The current generation
$mutRate\_max = min\{3 \times mutRate\_init, 0.9\}$;
$v = [n_d, R_s, R_{sh}]$; The chromosme structure
$pop = popGen(popSize)$; Random initial population of popSize

Step 2: Crossover and mutation

Selecting the parents ($\lambda = rand() \in [0,1]; i \in \{1,2\}$):
$[parent_{1,c}, parent_{2,c}] = RouletteWheel(crossoverRate)$;
$offspring_{i,c} = \lambda parent_{1,c} + (1-\lambda) parent_{2,c}$;
$mutRate = mutRate\_init + (mutRate\_max - mutRate\_init)(\frac{\overline{fitness_{genIndx}}}{fitness_{best,genIndx}})^a$;
Selecting the chromosomes/variable to be mutated:
$[chrom, var]_m = RouletteWheel(mutRate)$;
$mutVar = var_m \times rand() \times (1 - \frac{genIndx}{genNo\_max})$;
$migratedChrom_m = chrom_m(mutVar)$; using mutated var.
$pop = pop \cup \{offspring_{i,c}\} \cup \{migratedChrom_m\}$;

Step 3: Calculating fitness values (j is the chromosome number)

Calculating the values of objective functions:;
$(v_{mpp,stc}, i_{mpp,stc})$ = Solve Eq. (6) for STC with IPM;
$(v_{mpp,noct}, i_{mpp,noct})$ = Solve Eq. (6) for NOCT with IPM;
$[f_{1,j}, f_{2,j}]$ = Use these values acc. to Eqs. (7) and (8);
$normalizeFactor_1 = \underset{j\in[0,popSize]}{\text{maximize}} \{f_{1,j}\}$;
$normalizeFactor_2 = \underset{j\in[0,popSize]}{\text{maximize}} \{f_{2,j}\}$;
$fitness_j = \frac{0.5}{normalizedFactor_1} f_{1,j} + \frac{0.5}{normalizedFactor_2} f_{2,j}$; Eqs. (9), (11b) and (8)

Step 4: Selection

$P_{sel,j} = \frac{|fitness_j - \overline{fitness_{genIndx}}|}{fitness_{best,genIndx}}$; selection probability
$pop = RouletteWheel(P_{sel,j})$; new population of popSize

Step 5: Terminating criteria

If the $genIndx < genNo\_max$ AND $fitness_{best,genIndx} < 10000$ then
update the genInx and go to step 2
else the chromosome $[n_d, R_s, R_{sh}]$ with the $fitness_{best,genIndx}$
is the optimum solution. STOP.

Table 5 presents a pseudocode of the proposed GA for this study. The proposed GA adopts the disruptive selection method [36] to find the global optimum point. Traditional GAs allocate more trials to above-average chromosomes and do not guarantee convergence to the global optimum. Unlike traditional GAs, the disruptive selection, which is a more effective method, gives a higher probability to both the best and the worst chromosomes in a roulette wheel framework [36]. Fig. 5 (a) and (b) illustrate that the employed disruptive selection method keeps diversity of the chromosomes up to the last generation in order to be able to find the global optima. Red dots are MPPs estimated by different chromosomes of the last generation and the black stars indicate target values. From Fig. 5 (c), it can be seen that although the best fitness remains constant for several consecutive generations, which means the algorithm is vulnerable to premature convergence, the average fitness is variable. In other words, the proposed GA preserves the population diversity throughout different generations. Figs. 5 (d)-(f) show the diversity of each estimated parameter throughout different generations. From Figs. 5 (d)-(f), it can be seen that although majority of the chromosomes are converged to an optimum point, the proposed GA still searches other possible options up to the last generation.

Moreover, the proposed GA employs two other techniques to preserve the population diversity through the generations and prevent a premature convergence. First, a specific technique is used to adjust the

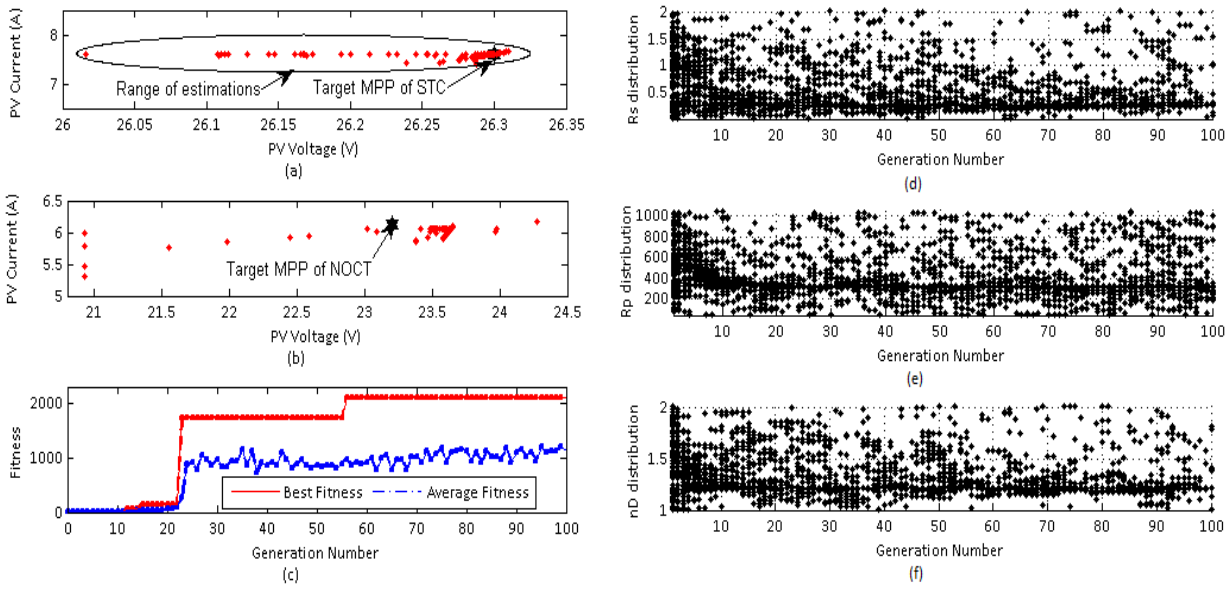

Figure 5: (a)-(b) Diversity of the estimated MPPs for different chromosomes of the last generation; (c) the average fitness which remains at the half of the best fitness throughout different generations with (d)-(f) the diversity of each estimated parameter in detail.

mutation rate dynamically. It changes the mutation rate proportionally to a diversity measurement, which is defined as the ratio of the average fitness to the best fitness [35]. Secondly, a random offspring generation strategy is used to preserve the population diversity. When two parents have equal genotypes, the normal offsprings are clone to their parents. The idea behind the random offspring generation strategy is that if this situation happens, then the normal offsprings are replaced by new randomly generated ones [37].

From Table 5 , it can be seen that the procedure calculates the maximum values of each objective function prior to selecting the chromosomes of the next population. These values are the normalization factors $\{\theta_i\}$ in Eq. (12) for each objective function.

Unlike the identification methods in [13] and [12], the proposed method does not require an initial guess for the ideality factor. The execution time is independent of the parameters resolution and the method can be terminated in the middle of the execution according to the accuracy-time trade-offs and having the sub-optimal solution.

4. Results, validation, and discussion

The proposed method is used to identify the equivalent electrical circuit of three PV modules with different technologies [38, 39, 40]. Table 1 illustrates the parameters of these PV modules provided by three manufacturers: Kyocera, Shell, and Sunpower. The following Subsection 4.1 presents identified model for the Sunpower E20/333 module using different variations of the proposed PV model identification method. It also validates the results of the proposed method by comparing them with the curves, available in the PV module datasheets [38, 39, 40]. Subsection 4.2 verifies the accuracy of the proposed MPP estimation algorithm with respect to the results of the prior researches. The obtained PV identification results are compared in Subsection 4.3 with two other studies in [13] and [28], indicating substantial improvements in accuracy. All the implementations are conducted using MATLAB with the following parameters:

- Design variables: $[n_d, R_s, R_{sh}]$
- The crossover rate: 85%
- The initial mutation rate: 40%
- The population size : 100

Table 6: The identified electrical parameters for Sunpower E20333 (Monocrystalline) module employing the proposed methods.

Parameters	**STC-based**	**NOCT-based**	**Full**
$n_d(-)$	1.132	1.014	1.167
$R_s(\Omega)$	0.365	0.598	0.337
$R_{sh}(\Omega)$	1125.75	1399.17	1414.89
The STC-identification error(%)	0.0004	1.6279	0.0121
The NOCT-identification error(%)	1.0927	0.0014	1.0208
The overall error(%)	**1.0931**	**1.6293**	**1.0375**

Table 7: The identified electrical parameters for the SHELL ST40 module (Thin film) and Kyocera KC200GT (Polycrystalline) modules employing the proposed methods.

	SHELL ST40			**Kyocera KC200GT**		
Parameters	**STC-based**	**NOCT-based**	**Full**	**STC-based**	**NOCT-based**	**Full**
$n_d(-)$	1.346	1.829	1.973	1.291	1.033	1.348
$R_s(\Omega)$	1.508	1.151	1.067	0.232	0.421	0.214
$R_{sh}(\Omega)$	386.22	294.59	510.49	547.91	662.813	1060.66
The STC-identification error(%)	0.0087	3.2138	3.0240	0.0007	3.1924	0.0291
The NOCT-identification error(%)	4.4390	0.0020	0.0210	2.190	0.0030	2.0960
The overall error(%)	**4.4477**	**3.2158**	**3.0450**	**2.191**	**3.1958**	**2.1254**

- The maximum number of generations: 100
- The affine weights: $[0.5, 0.5]$

4.1. The Sunpower E20/333 model identification and validation

Table 6 presents the electrical parameters of the Sunpower E20/333 PV module identified by different variations of the proposed method. It shows a comparison between different errors in STC-based, NOCT-based, and full methods indicating how the full method provides a solution with better overall error, with respect to the MPPs (Table 1), than the other variations (with 5.1% improvement). The identified solution by the full method is close to the results of the STC-based method, however, it is not necessarily the same for other types of the PV modules. From Table 7, it can be seen for the ST40 module that the identified solution by the full method is much closer to the results of the NOCT-based method and it experiences an improvement of 31.5% compared with the STC-based method.

Fig. 6 compares the predicted $I-V$ curves of the E20/333 PV module for different amounts of the solar irradiance and the cell temperature with the points provided by the manufacturer (the circle markers). It is observed that the identified model by the proposed full method predicts different curves so that they are very close to the manufacturer's provided points.

Fig. 7 depicts the *curve error* versus the PV voltage for different amounts of solar irradiance. The curve error is defined as the absolute normalized difference between the predicted $I-V$ curve, which is generated by employing the identified model, and the $I-V$ curves which is provided by manufacturers. If there exist predicted and manufacturer provided points with the same value of the voltage (or current) on the curves, then the error equals to the absolute difference between the proportional current (or voltage) values. The calculated absolute values are normalized with either the short-circuit current or open-circuit voltage values.

4.2. The MPP estimation algorithm verification and validation

The MPP estimation algorithm is validated with the results of the curve-investigating method [13] that finds the MPP with any required accuracy employing an exhaustive search. Table 8 compares the estimated MPPs for the STC and NOCT curves using either of these methods. The results show that they are match together precisely and the proposed algorithm estimates the MPP quite accurately comparing with the manufacturer values (Table 1).

4.3. Accuracy verification of the proposed method

From Figures 6 and 7 and the explanations under subsections 4.1 and 4.2, it can be seen that the proposed method extracts a PV model that predicts accurately matched $I-V$ curves to the curves available

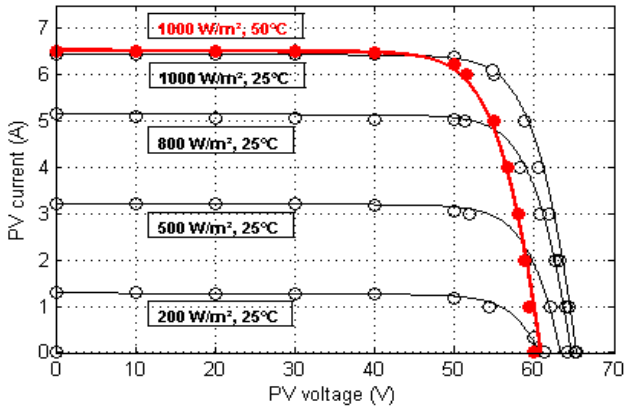

Figure 6: The predicted $I-V$ curves (the solid lines) and the manufacturer's points (the circle markers) of the Sunpower $E20/333$ PV module for different values of solar irradiance and $T_c = 25°C$, in addition to the case that $T_c = 50°C$ (the thicker line and the solid circle markers).

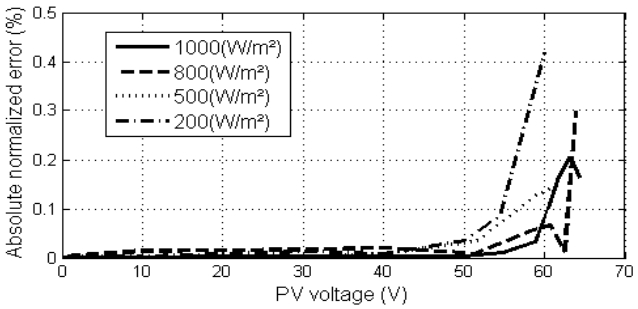

Figure 7: The absolute normalized curve errors between the predicted and manufacturer provided $I-V$ curves of the E20/333 module at different amounts of the solar irradiance.

by the manufacturers. In order to indicate the improved accuracy of the proposed method, the measured identification error, as the sum of the STC- and the NOCT-identification errors, is also compared with the corresponding values introduced by the methods in [13] and [28]. Fig. 8 shows this comparison for different PV modules. It is observed that the identified model by the proposed full method generates the least overall error among all methods. For instance, applying the proposed full method for the KC200GT and ST40 modules comparing with the results in [13] and [28] delivers a significant improvement of 20.8% and 46.3%, respectively. Identically, dramatic improvements of 99.7% and 98.3% with respect to these references are gained for the STC-identification errors when the STC-based method is applied to these two modules.

The absolute normalized curve error between the predicted and manufacurer provided $I-V$ curves of ST40 module for two different values of insolation are given in Fig. 9. The absolute errors have been normalized using similar technique introduced under Fig. 7. From Fig. 9, the proposed full method shows a significant reduction in curve errors and especially it gives dramatic improvements for lower insolations.

Table 8: The comparison between the proposed MPP estimation algorithm and the curve-investigating method [13].

	KC200GT		**ST40**		**E20/333**	
Methods	**STC**	**NOCT**	**STC**	**NOCT**	**STC**	**NOCT**
Curve-investigating method: $\binom{V_{mpp}}{I_{mpp}}$	$\binom{26.3000}{7.6100}$	$\binom{23.2000}{6.1300}$	$\binom{16.5980}{2.4100}$	$\binom{14.7030}{1.8840}$	$\binom{54.7000}{6.0900}$	$\binom{50.4000}{4.9100}$
The proposed method: $\binom{V_{mpp}}{I_{mpp}}$	$\binom{26.3001}{7.6099}$	$\binom{23.1994}{6.1300}$	$\binom{16.5990}{2.4099}$	$\binom{14.7000}{1.8844}$	$\binom{54.7002}{6.08999}$	$\binom{50.4002}{4.9099}$

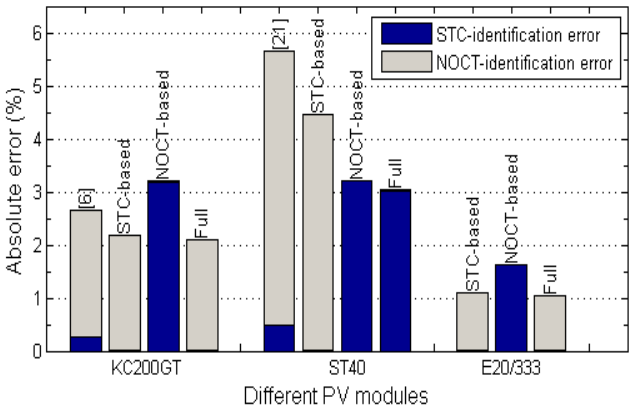

Figure 8: The identification error of the proposed methods comparing with the results in [13] and [28].

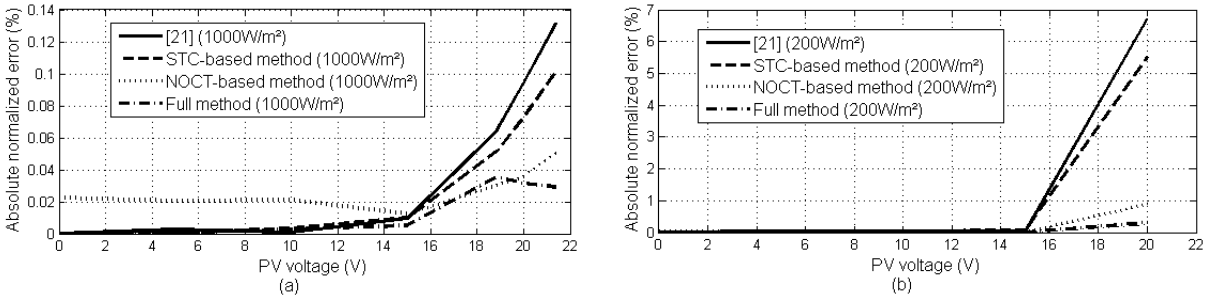

Figure 9: The absolute normalized curve errors between the predicted and manufacturer provided $I-V$ curves of the ST40 module introduced by different methods at (a) $1000W/m^2$ and (b) $200W/m^2$ insolation.

The introduced improvement by applying the proposed full method may vary for different types of the PV modules; however, the full method is still a consistent identification algorithm. It means that it always proposes the optimum solution with respect to the overall and curve errors, regardless of the different PV technologies. A PV module is dominated by either the NOCT (e.g. the ST40 module) or the STC condition (e.g. the KC200GT or the E20/333 modules). If it is dominated by the NOCT condition, using the STC-based identification method (e.g. the methods in [13] and [28]) provides a model with significant overall error chiefly because of a substantial NOCT-identification error. The proposed full method is consistent, i.e., it automatically adjusts itself to find the best equivalent electrical model for a PV module, regardless of being dominated by either the STC or the NOCT condition.

5. Conclusion

This paper proposes a method to identify the parameters of the PV modules equivalent electrical circuits. The identified model is essential to simulate the behavior of the PV modules at any operating condition. The main aspect of the proposed model identification method is to extract the electrical parameters with minimizing the overall identification error rather than just the STC-identification error. While the latter is the distance between the estimated and manufacturer provided MPPs of the STC curve, the overall identification error is the sum of such distances for both the STC and the NOCT curves. The PV identification has been reformulated as a nonlinear optimization problem. A novel GA has been introduced to solve the resulting multi-objective global optimization problem, which has several local optima. In order to estimate the MPP of a given $I-V$ curve, which is a subproblem of the main PV identification problem, a novel MPP estimation algorithm has also been proposed. Unlike the prior approaches that construct a set of points of

the $I-V$ curve, the proposed fast MPP estimation algorithm employs IPM to extract directly the MPP.

By applying the proposed identification method to three PV modules of different thin film, polycrystalline, and monocrystalline technologies, the overall errors against manufacturers data are improved by a factor between 5.1% to 31% depending on the PV technology. It indicates that the proposed method works well even for the PV modules dominated by the NOCT condition. The identified models for Kyocera KC200GT and SHELL ST40 PV modules are also compared with the results provided by two recent researches and show considerable improvements of respectively 20.8% and 46.3%. Moreover, by employing IPM, the proposed method is up to 10 times faster than prior methods. The pseudocode of the proposed PV model identification algorithm and a sample MATLAB script of the developed MPP estimation algorithm are presented.

Acknowledgement

The authors would like to thank the Synchron Technology Ltd. for their financial support of this research.

Appendix A: The interior-point method

A nonlinear constrained optimization problem can be defined as follows:

$$\underset{z\in\Re^n}{\text{minimize}} \quad F(z) \tag{13a}$$

$$\text{subject to:} \quad G(z)=0 \tag{13b}$$

$$H(z)\geq 0. \tag{13c}$$

where the vector of functionals G and H are the equality and inequality constraints of the problem, respectively. The fundamental idea of the IPM is to modify this problem under consideration that all constraints become equality constraints. There are two main approaches to achieve this aim, namely, the *homotopy method*, and the *barrier method*. Here, a summary of the former approach has been provided and reader is referred to [31] and [32] for further details.

According to the homotopy method all inequality constraints are converted to equality ones using a vector of slack variables s so then Eq. (13) is transformed to Eq. (14) as follows:

$$\underset{z\in\Re^n, s\in\Re^{n_s}}{\text{minimize}} \quad F(z) \tag{14a}$$

$$\text{subject to:} \quad G(z)=0 \tag{14b}$$

$$H(z)-S=0. \tag{14c}$$

where n_s is the dimension of the slack variables equals to the number of inequality constraints and $S=diag(s)$. Now applying the KKT theorem a system of differential and algebraic equations are constructed as the necessary conditions. The theorem states that for an optimal point z^* of Eq. (14) there exist multipliers λ^* and μ^* and the slack variables s^* such that the system of equations:

$$\nabla_z \mathscr{L}(w^*,\lambda^*,\mu^*)=0 \tag{15a}$$

$$S\mu-\nu e=0 \tag{15b}$$

$$G(z^*)=0 \tag{15c}$$

$$H(z^*)-S=0 \tag{15d}$$

$$s^*\geq 0. \tag{15e}$$

holds where $e=[1,1,...,1]^T$, υ is an iteratively vanishing perturbation parameter ($\lim_{j\longrightarrow\infty}\upsilon_j=0$) in order to enforce the solution to stay away from the boundaries, and $\mathscr{L}$ is the Lagrangian function of (14) as follows:

$$\mathscr{L}(z, \lambda, \mu) = F(z) - G(z)^T \lambda - H(z)^T \mu. \tag{16}$$

Now the methods such as the linesearch or trust-region can be employed to solve Eq. (15) iteratively to find the set of $(z^*, \lambda^*, \mu^*, s^*)$.

Appendix B: MATLAB scripts

Table 9 illustrate a summary of the MATLAB scripts for the proposed MPP estimation algorithm.

Table 9: MATLAB scripts of the proposed MPP estimation algorithm.

```
%The objective function and the constraints must be in separate files.

iph = iph_STC;
a_Tc = a_STC;
i0 = i0_STC;

% The solve for the optimization problem
x0 = [voc_STC * 0.8, isc_STC * 0.7];      %initial guess
opt_lb = [voc_STC * 0.5, isc_STC * 0.5]; %lower bounds
opt_ub = [voc_STC, isc_STC];              %upper bounds
options = optimset('Algorithm','interior-point', 'TolFun', ...
                   1e-18, 'Display', 'off');
[ x,fval ] = fmincon(@PVObj,x0,[],[],[],[],opt_lb ...
                opt_ub,@(x)PVConstraints(x, var3, iph_STC,...
                     i0_STC, var1, var2, a_STC/var3),options);
[ c, ceq ] = confun(x);
vmpp = x(2); impp = x(1); pmpp = vmpp * impp;

% The objective function
function f = PVObj(x)
    f = 1/(x(1) * x(2));
end

% The constraints function
function [ c, ceq ] = PVConstraints(x, nd, iph, i0, rs, rsh, vt)
    % Nonlinear equality constraints
    c = [];
    % inequality constraints
    ceq = [(x(1) - iph +...
          i0 * (exp(( rs * x(1) + x(2)) / (nd * vt)) - 1) +...
          ((rs * x(1) + x(2)) / rsh)) ] ;
end
```

References

[1] J. L. Agorreta, M. Borrega, J. Lopez, and L. Marroyo. Modeling and Control of N-Paralleled Grid-Connected Inverters With LCL Fitler Coupled Due to Grid Impedance in PV Plants. *IEEE Transactions on Power Electronics*, 26(3):770–785, 2011.

[2] F. Locment, M. Sechilariu, and I. Houssamo. DC Load and Batteries Control Limitations for Photovoltaic Systems. Experimental Validation. *Power Electronics, IEEE Transactions on*, 27(9):4030 –4038, sept. 2012. ISSN 0885-8993.

[3] A. M. Dizqah, A. Maheri, K. Busawon, and P. Fritzson. Acausal Modelling and Dynamic Simulation of the Standalone Wind-Solar Plant Using Modelica. In *IEEE 15th International Conference on Computer Modelling and Simulation (UKSim2013)*, pages 580–585, Cambridge, UK, April 2013.

[4] P. E. Kakosimos, and A. G. Kladas. Implementation of Photovoltaic Array MPPT Through Fixed Step Predictive Control Technique. *Renewable Energy*, 36:2508–2514, 2011.

[5] A. Kouchaki, H. Iman-Eini, B. Asaei. A new maximum power point tracking strategy for {PV} arrays under uniform and non-uniform insolation conditions. *Solar Energy*, 91(0):221 – 232, 2013. ISSN 0038-092X.

[6] K. Ishaque, Z. Salam, M. Amjad, and S. Mekhilef. An Improved Particle Swarm Optimization (PSO)-Based MPPT for PV With Reduced Steady-State Oscillation. *IEEE Transactions on Power Electronics*, 27(8):3627–3638, 2012.
[7] T. Bennett, A. Zilouchian, R. Messenger. A proposed maximum power point tracking algorithm based on a new testing standard. *Solar Energy*, 89(0):23 – 41, 2013. ISSN 0038-092X.
[8] M. K. Deshmukh, and S. S. Deshmukh. Modelling of Hybrid Renewable Energy System. *Renewable And Sustainable Energy Reviews*, 12:235–249, 2008.
[9] E. Karatepe, M. Boztepe, and M. Colak. Development of a Suitable Model for Characterizing Photovoltaic Arrays with Shaded Solar Cells. *Journal of Solar Energy*, 81:977–992, 2007.
[10] A. Mellit, and S. A. Kalogirou. ANFIS-Based Modelling for Photovoltaic Power Supply System: A Case Study. *Journal of Renewable Energy*, 36:250–258, 2011.
[11] J. A. Gow, and C. D. Manning. Development of a Photovoltaic Array Model for Use in Power-Electronics Simulation Studies. In *Proc. IEE Electric Power Applications*, volume 146, pages 193–200, 1999.
[12] K. Ishaque, Z. Salam, and H. Taheri. Simple, Fast and Accurate Two-Diode Model for Photovoltaic Modules. *Journal of Solar Energy Materials and Solar Cells*, 95:586–594, 2011.
[13] M. G. Villalva, J. R. Gazoli, and E. R. Filho. Comprehensive Approach to Modeling and Simulation of Photovoltaic Arrays. *IEEE Transactions on Power Electronics*, 24(5):1198–1208, 2009.
[14] J. Martinez, and A. Medina. A State Space Model for the Dynamic Operation Representation of Small-Scale Wind-Photovoltaic Hybrid Systems. *Journal of Renewable Energy*, 35:1159–1168, 2010.
[15] G. Walker. Evaluating MPPT Converter Topologies Using a Matlab PV Model. *Journal of Electrical and Electronics Engineering*, 21:45–55, 2001.
[16] A. N. Celik, and N. Acikgoz. Modelling and Experimental Verification of the Operating Current of Mono-Crystalline Photovoltaic Modules Using Four- and Five-Parameter Models. *Journal of Applied Energy*, 84:1–15, 2007.
[17] D. S. H. Chan, and J. C. H. Phang. Analytical Methods for the Extraction of Solar-Cell Single- and Double-Diode Model Parameters from I-V Charactristics. *IEEE Transactions on Electron Devices*, ED-34:286–293, 1987.
[18] W. De Soto, S. A. Klein, and W. A. Beckman. Improvement and Validation of a Model for Photovoltaic Array Performance. *Journal of Solar Energy*, 80:78–88, 2006.
[19] D. Sera, R. Teodorecu, and P. Rodriguez. PV Panel Model Based on Datasheet Values. In *Proc. IEEE Int. Symp. Electronic*, pages 2392–2396, 2007.
[20] A. Chaterjee, A. Keyhani, and D. Kapoor. Identification of Photovoltaic Source Models. *IEEE Transactions on Energy Conversion*, 80:78–88, 2011.
[21] R. Kardi, H. Andrei, J. P. Gaubert, T. Ivanovici, G. Champenois, and P. Andrei. Modeling of the Photovoltaic Cell Circuit Parameters for Optimum Connection Model and Real-Time Enulator with Partial Shadow Conditions. *Journal of Energy*, 42:57–67, 2012.
[22] M. Zagrouba, A. Sellami, M. Bouaicha, and M. Ksouri. Identification of PV Solar Cells and Modules Parameters Using the Genetic Algorithms: Application to Maximum Power Extraction. *Journal of Solar Energy*, 84:860–866, 2010.
[23] F. M. Petcut, and T. L. Dragomir. Solar Cell Parameter Identification Using Genetic Algorithms. *Journal of Control Engineering and Applied Informatics*, 12:30–37, 2010.
[24] D. L. King, W. E. Boyson, and J. A. Kratochvil. Photovoltaic Array Performance Model. Technical Report SAND2004-3535, Sandia National Laboratories, 2004.
[25] U. Stutenbaeumer, and B. MEsfin. Equivalent Model of Monocrystalline, Polycrystalline and Amorphous Silicon Solar Cells. *Journal of Renewable Energy*, 18:501–512, 1999.
[26] SNL. Sandia National Laboratories. www.sandia.gov.
[27] NIST. National Institute of Standards and Technology. www.nist.gov.
[28] J. J. Soon, and K. S. Low. Photovoltaic Model Identification Using Particle Swarm Optimization With Inverse Barrier Constraints. *IEEE Transactions on Power Electronics*, 27:3975–3983, 2012.
[29] Q. Kou, S. A. Klein, and W. A. Beckman. A Method for Estimating the Long-Term Performance of Direct-Coupled PV Pumping Systems. *Journal of Solar Energy*, 64:33–40, 1998.
[30] IPOPT. Interior Point OPtimizer. www.projects.coin-or.org/Ipopt.
[31] S. Boyd,L. Vandenberghe. *Convex Optimization*. Cambridge University Press, New York, 2004.
[32] L. T. Biegler. *Nonlinear Programming: Concepts, Algorithms, and Applications to Chemical Processes*. The society for industrial and applied mathematics and the mathematical optimization society, Philadelphia, 2010.
[33] R. T. Marler, and J. S. Arora. Survey of Multi-Objective Optimization Methods for Engineering. *Journal of Structural Multidisciplinary Optimization*, 26(6):369–395, 2004.
[34] A. Konak, D. W. Coit, A. E. Smith. Multi-Objective Optimization Using Genetic Algorithms: A Tutorial. *Journal of Reliability Engineering And System Safety*, 91:992–1007, 2006.
[35] M. Gen, and R. Cheng. *Genetic Algorithms and Engineering Design*. J. Wiley And Sons, New York, 2000.
[36] T. Kuo, and S. Y. Hwang. A Genetic Algorithm with Disruptive Selection. *IEEE Transactions on Systems, Man, And Cybernetics*, 26(2):299–307, 1996.
[37] M. Rocha, and J. Neves. Preventing Premature Convergence to Local Optima in Genetic Algorithms Via Random Offspring Generation. In *IEA/AIE '99 Proceedings of the 12th Int'l. Conference on Industrial and Engineering Applications of Artificial Intelligence and Expert Systems: Multiple Approaches to Intelligent Systems*, pages 127–136. Springer-Verlag, 1999.
[38] Kyocera. KC200GT, High Efficiency Multicrystal Photovoltaic Module. www.kyocerasolar.com/assets/001/5195.pdf, 2012.
[39] SHELL. Shell ST40 Photovoltaic Solar Module. www.oeko-energie.de/prospekte/ShellST40_D.pdf, 2012.

[40] Sunpower. High Efficiency Home Solar Panels - E20 Series. www.sunpowercorp.co.uk/homes/products-services/solar-panels/e20, 2012.